Maus, S., Rother, M., Holme, R. T., Lühr, H., Olsen, N., Haak, V. (2002): First scalar magnetic anomaly map from CHAMP satellite data indicates weak lithospheric field. - Geophysical Research Letters, 29, 14,

DOI: 10.1029/2001GL013685

Geophysical Research Letters, in print

First scalar magnetic anomaly map from CHAMP satellite data indicates weak lithospheric field

S. Maus, M. Rother, R. Holme, H. Lühr, N. Olsen[1], and V. Haak

GeoForschungszentrum Potsdam, Germany

Abstract. Satellite magnetic anomaly maps derived by different techniques from Magsat/POGO data vary by more than a factor of 2 in the deduced strength of the lithospheric magnetic field. Here, we present a first anomaly map from new CHAMP scalar magnetic field data. After subtracting a recent Ørsted main and external field model, we remove remaining unmodeled large-scale external contributions from 120° track segments by subtracting a best-fitting uniform field. In order to preserve N/S trending features, the data are not filtered along-track. Direct integration of the spherically gridded data yields the final degree 14-65 spherical harmonic expansion of the total intensity anomaly at the mean satellite altitude of 438 km. Apart from enhanced long wavelength features and a smoother general appearance, our initial map is strikingly similar to one of the lower strength Magsat/POGO maps.

Introduction

Magnetic anomaly maps derived from ship and airborne surveys have played a key role in unraveling the structure and dynamics of the Earth's lithosphere. However, magnetic anomalies with wavelengths of more than 500 km are not reliably determined by the stitching together of such near surface surveys. Only satellites can provide the global perspective. The POGO (1967-1971) and Magsat (1979-1980) missions proved that the weak lithospheric magnetic field is indeed discernible at satellite altitude. Due to high noise levels and eccentric orbits, lithospheric field models derived by different techniques from the early satellite data, namely CWKS89 [*Cain et al.*, 1989], CA90 [*Cohen and Achache*, 1990], ALP94 [*Arkani-Hamed et al.*, 1994] and CM3 [*Sabaka et al.*, 2000], disagree considerably. In particular, the overall strength of the lithospheric field differs between the various models by more than a factor 2, corresponding to a factor 4 difference in the power spectra (Fig 1).

After 20 years without suitable measurements, CHAMP was launched in July 2000 into a nearly circular, polar orbit with an initial altitude of 455 km, decaying to 300 km over a life span of 5 years (see http://op.gfz-potsdam.de/champ for details). Our analysis of scalar data from the first 14 months of the mission provides strong evidence in favor of a relatively weak lithospheric field. The lithospheric magnetic anomaly map exhibits remarkable similarity to the combined Magsat/POGO map ALP94 of *Arkani-Hamed et al.* [1994].

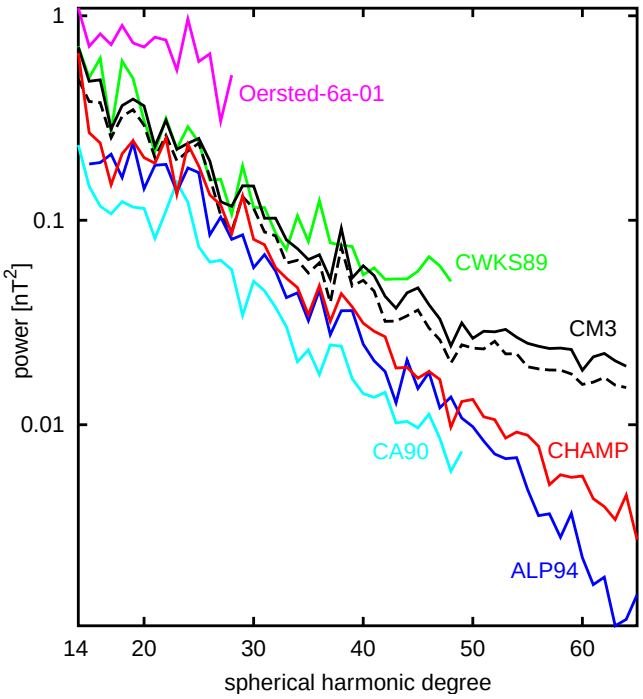

Figure 1. Power spectra of the total intensity anomaly (definition of *Arkani-Hamed et al.* [1994, eq. 6]) at 450 km altitude of several Magsat and POGO lithospheric field models, together with the spectrum of our new CHAMP map. ALP94 and CHAMP were upward continued by 50 km and 12 km, respectively. The dashed line indicates the loss of power if the same external field correction and gridding procedure which we used for the CHAMP data is applied to equivalent sample tracks from the CM3 model.

[1] Danish Space Research Institute, Copenhagen, Denmark

Data Selection

From the CHAMP scalar proton magnetometer data, covering the period of 9 Aug. 2000 to 30 Sep. 2001, we extract overlapping track segments of 120° in length centered about the equator (low latitude) and of 100° in length centered about each of the poles. For the low latitudes we select the night time data from 22:00 to 6:00 local time (LT). The period of 19:00 to 22:00 LT is excluded due to significant small-scale structure in the data which we attribute to F region currents, addressed in a separate paper [*Lühr et al.*, 2001]. Plotting the mean rms residuals after main and external field corrections against K_p, we find $K_p \leq 2$ to be a suitable criterion for magnetic activity. For the polar data we initially select all data, irrespective of local time, season or K_p. From each of the three sets of tracks we then select a dense, undisturbed coverage by rejecting those tracks which have neighbors with significantly lower mean residual rms on both sides. Typical mean residuals of undisturbed tracks are 0.5 nT to 5 nT for low latitudes and 2 nT to 8 nT for polar latitudes. To account for gradients in the lithospheric field, tracks are only rejected if the rms difference to both neighbors exceeds $0.25\Delta\varphi + threshold$, where $\Delta\varphi$ is the equatorial track separation in degrees longitude. We find that thresholds of 0.5 nT for low latitude and 1 nT for polar segments provide an optimum undisturbed coverage, consisting of 1765 low latitude, 458 North Polar and 440 South Polar tracks.

Data Processing

The low latitude and polar track segments are processed separately by the following scheme and the residuals are merged in the spherical gridding, using a 20° roll-off weight function in the overlap. The final model is given by degrees 14-65 of the spherical harmonic expansion of the grid.

Removal of main and external fields

To account for the main field we use the model Ørsted-06a-01 [*Olsen*, 2002]. This model extends to degree 29, with linear secular variation up to degree 13, a degree 2 external field with annual and semi-annual contributions and a degree 1 D_{st} dependent part. Degrees 15-29 of the model (see power spectrum in Fig 1) represent the lithospheric field and are therefore not used here. Figure 2 displays the residuals, after subtracting the main (up to degree 14) and external field, for a sample of tracks crossing the equator near 20° longitude. As experienced with Magsat and POGO data [*Langel and Hinze*, 1998], the contribution to the residual from unmodeled external fields is stronger than the lithospheric signal to be extracted. Some authors have used along-track high pass filters to deal with the problem. A known caveat of these filters is that they remove genuine N/S trending lithospheric anomalies [*Purucker and Dyment*, 2000]. Instead of using filters, other groups have therefore improved external field corrections by including additional observatory data [*Cain et al.*, 1989; *Sabaka et al.*, 2000]. The latter approach leads to lithospheric field models with 4 times the power of the models from filtered data (Fig 1). Arguably, dealing with external fields is the most difficult issue in the extraction of the lithospheric signal.

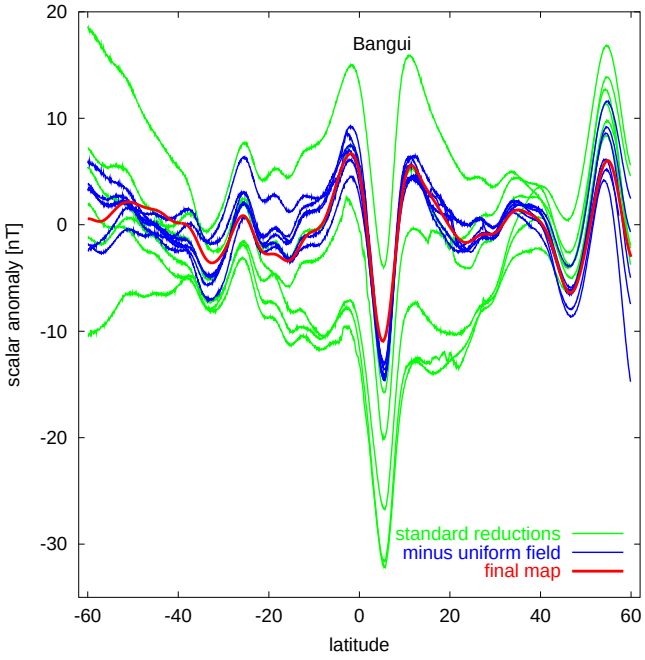

Figure 2. Night time sample tracks at 20.0°-20.7° longitude. After the standard D_{st} correction, the remaining residuals (green) are still dominated by external fields. In order to retain as much along-track signal as possible, we only subtract a best fitting homogeneous field from each track (result shown in blue), instead of the usual along-track filtering. Note the signature of the well known Bangui anomaly at 5°N. Underestimation of this peak by our final map (red) is due to truncation at spherical harmonic degree 65.

The contribution of magnetospheric currents to a short track segment of 120 degrees in length (30 min. flight time) is well represented by a homogeneous, uniform field because the distance between the satellite and the source currents is several Earth radii. We estimate the 3 free parameters of this uniform field in an Earth fixed frame, separately for each track segment, by minimizing the rms residual of the total intensity anomaly. Subtracting this first order estimate of the external field significantly improves the agreement be-

tween nearby tracks (Fig. 2). To investigate the possible unintended removal of genuine lithospheric signal by this correction procedure we have processed the lithospheric part of model CM3 by the same procedure as the CHAMP data. The spectrum of the result (dashed in Fig 1) indicates that some lithospheric signal is indeed lost in the correction. However, the effect is small compared with the differences between the various lithospheric field models. Figure 3 shows that there is a general agreement between the external field correction estimated from CHAMP data and the correction according to the provisional D_{st} index. Nevertheless, the deviation is still of the order of 10 nT which is several times the mean lithospheric field strength.

Spherical harmonic expansion

Here, we derive a spherical harmonic expansion of the total intensity for a median altitude of 438 km. In fact, 50% (75%) of the data were acquired at altitudes of 439 ± 15 km (441 ± 22 km) and 95% of the data belong to the range of 443 ± 33 km above the reference sphere with $r = 6371.2$ km. Because of the low eccentricity of CHAMP's orbit, deviations from the average orbit altitude can be ignored. Indeed, *Cain et al.* [1989] use this approach even for Magsat with its much more eccentric orbit. For the future, we plan to estimate the spherical harmonic coefficients of the magnetic potential directly from the precisely located data set of residuals. However, the inherent non-uniqueness of the inverse problem for scalar data [*Backus*, 1970], the large amount of data points and the uneven spatial coverage lead to difficulties which are beyond the scope of the present study.

We grid the residuals on a spherical surface at 438 km altitude. To every grid point we assign the weighted average of the data points located within a distance of $d = 100$ km using the weight function $(0.5 + 0.5\cos(\pi d/100\ \mathrm{km}))^2$. The window size is expanded at the poles in order to fill in the 2.7° gaps. Subsequently, the spherical harmonic coefficients of the total intensity anomaly are found by direct integration. In the presence of a strong dipolar main magnetic field, a weak super-imposed lithospheric field with a potential of harmonic degree ℓ contributes mostly to degree $\ell - 1$ and partly to degree $\ell + 1$ of the total intensity anomaly [*Arkani-Hamed et al.*, 1994]; see *Maus* [2001, p. 29] for a proof. Having subtracted a main field model of degree 14, degrees 1-13 of the total intensity anomaly have little power and are set to zero. We truncate the model above degree 65, since wavelengths shorter than 600 km are not reliably determined in the present analysis. With more data as the CHAMP mission continues and the altitude decreases, we anticipate being able to expand the model to higher degrees.

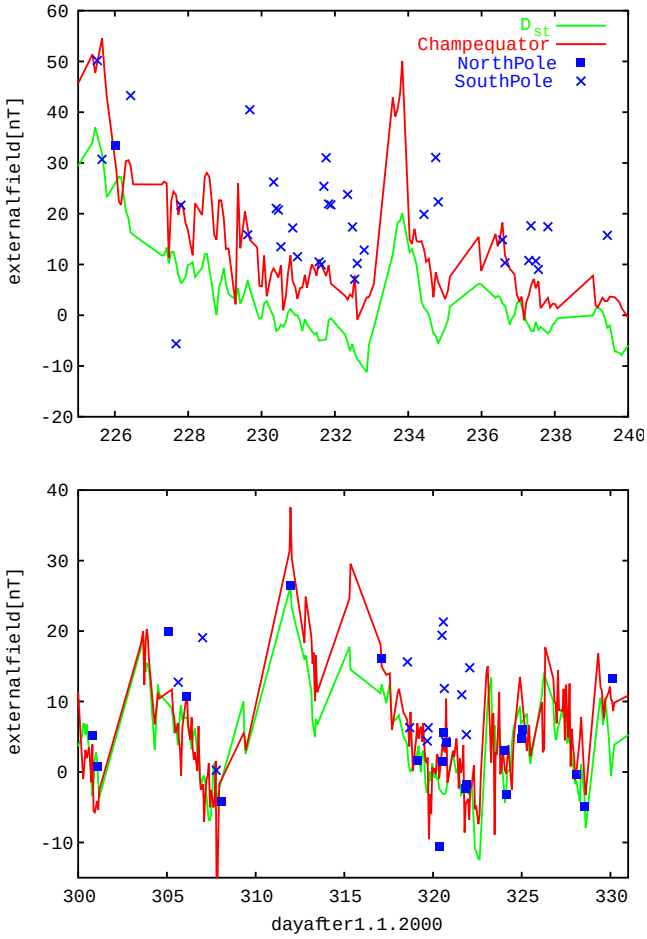

Figure 3. Strength of the external field component parallel to the Earth's rotation axis for 2 representative time periods. The green line shows the value obtained by multiplying the provisional D_{st} index with the empirically derived coefficient of -0.7 from the Ørsted-06a-01 model. Our estimate from CHAMP track segments is given as a red line for low latitudes, as crosses for the South Polar, and as squares for the North Polar region. At mid latitudes the D_{st} index tracks reasonably well the variations of the external field but sometimes exhibits baseline shifts of the order of 10 nT, several times stronger than the mean lithospheric field.

Results

The resulting total intensity anomaly map (Fig. 4) is consistent with many of the features seen in the Magsat/POGO model ALP94, in particular, the contrast between a weakly magnetized oceanic and a strongly magnetized continental lithosphere, scaling with the strength of the main field in a non-trivial way. In fact, the magnetization in the Pacific turns out to be even weaker than previously assumed, with

some notable exceptions in the west. Our map gives an improved account of the long crustal wavelengths, as is apparent in the Atlantic Ocean and in the Arctic, where structures are well aligned with the Mid Ocean Ridge. We also see N/S trending anomalies in the South Atlantic; consistent with the recent study of *Purucker and Dyment* [2000].

Surprisingly, anomaly amplitudes over the Arctic Ocean are higher than over Antarctica. Magsat and Ørsted have gaps of 7° in radius at the poles, which raised questions about the reliability of the earlier field models in the polar caps. It is therefore remarkable that a large positive anomaly in the American sector of the Arctic Ocean close to the North Pole, present in ALP94, CWKS89 and CM3, has now been confirmed by CHAMP with its polar gap of only 2.7°. On the other hand, large Antarctic anomalies given by CM3 and CWKS89 have not been confirmed. They may be due to auroral ionospheric currents because the Magsat mission was confined to the Antarctic summer.

Conclusions and outlook

The primary challenge in mapping the lithospheric magnetic field by satellite is the correction for external fields. While the influence of ionospheric currents can be almost entirely avoided by selecting quiet night time data (low latitudes) or tracks with low residual rms (polar latitudes), variable contributions from the magnetosphere are always present and are only partly removed by the usual D_{st} correction. In some earlier studies this problem was not fully addressed, leading to an overestimation of lithospheric field strength. On the other hand, along track filtering, linear detrending and the fitting and removal of external field models from individual tracks carries the danger of eliminating genuine along-track lithospheric signal. Consequently, only the across-track signal is fully preserved, resulting in E/W trending stripes which are clearly visible in some maps. At the moment, the ambiguity between large scale external fields and N/S trending lithospheric anomalies cannot be resolved entirely. Here, we have avoided along track filtering by subtracting a homogeneous background field from track segments spanning 1/3 of an orbit. Considerable improvement in the external field modeling is expected from the CHAMP vector data. Eventually, a simultaneous joint inversion of CHAMP, Ørsted, SAC-C and observatory data is likely to yield the best results.

In summary, a straight forward analysis of first CHAMP scalar magnetic field data has already resulted in a significant clarification of the global anomaly map. A continuous flow of high quality data from CHAMP, Ørsted and SAC-C is currently opening a new era in the mapping of lithospheric magnetic anomalies. Combined with continental scale aeromagnetic compilations, these maps provide a new basis for studies of crustal structure, dynamics and heat flow.

Acknowledgments. Helpful comments from an anonymous reviewer are gratefully acknowledged. Figure 4 was prepared with GMT. CHAMP is supported by DLR under FKZ 50 EP 9587.

References

Arkani-Hamed, J., R. A. Langel, and M. Purucker, Scalar magnetic anomaly maps of Earth derived from POGO and Magsat data, *J. Geophys. Res.*, *99*, 24,075–24,090, 1994.

Backus, G. E., Non-uniqueness of the external geomagnetic field determined by surface intensity measurements, *J. Geophys. Res.*, *75*, 6339–6341, 1970.

Cain, J. C., Z. Wang, C. Kluth, and D. R. Schmitz, Derivation of a geomagnetic model to n = 63, *Geophys. J. Int.*, *97*, 431–441, 1989.

Cohen, Y., and J. Achache, New global vector magnetic anomaly maps derived from Magsat data, *J. Geophys. Res.*, *95*, 10,783–10,800, 1990.

Langel, R. A., and W. J. Hinze, *The magnetic field of the Earth's lithosphere - The satellite perspective*, Cambridge Univ. Press, 1998.

Lühr, H., S. Maus, M. Rother, and D. Cooke, First in situ observation of night time F region currents with the champ satellite, *Geoph. Res. Lett.*, *in print*, 2001.

Maus, S., *New statistical methods in gravity and magnetics*, Habilitation thesis, University of Braunschweig, http://www.gwdg.de/∼smaus/habil.pdf, 2001.

Olsen, N., A model of the geomagnetic main field and its secular variation for epoch 2000 estimated from Ørsted data, *Geophys. J. Int.*, *in print*, 2002.

Purucker, M. E., and J. Dyment, Satellite magnetic anomalies related to seafloor spreading in the South Atlantic Ocean, *Geophys. Res. Lett.*, *27*, 2765–2768, 2000.

Sabaka, T. J., N. Olsen, and R. A. Langel, A comprehensive model of the near-Earth magnetic field: phase 3, *Technical Report, NASA/TM-2000-209894*, 2000.

S. Maus, GeoForschungszentrum Potsdam, Telegrafenberg, 14473 Potsdam, Germany, smaus@gfz-potsdam.de

This preprint was prepared with AGU's LaTeX macros v5.01, with the extension package 'AGU++' by P. W. Daly, version 1.6b from 1999/08/19.

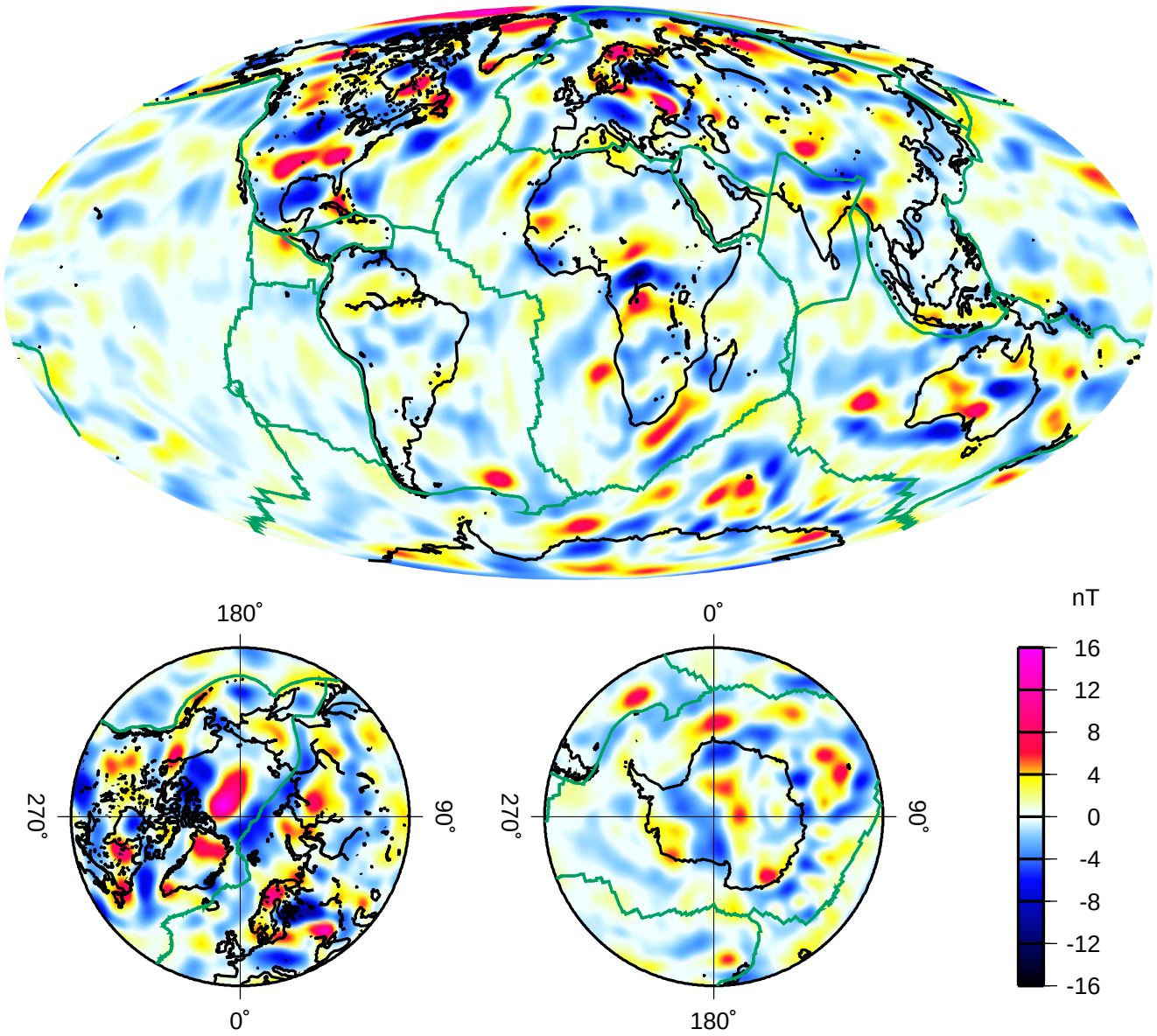

Figure 4. CHAMP scalar magnetic anomaly at 438 km altitude. The color scheme emphasizes weak anomalies.